Electronic Supplementary Information

Extended gate-type organic transistor functionalized by molecularly imprinted polymer for taurine detection

Qi Zhou, Mengqiao Wang, Shunsuke Yagi and Tsuyoshi Minami*

Institute of Industrial Science, The University of Tokyo, 4-6-1 Komaba, Meguro-ku, Tokyo, 153-8505, Japan.

E-mail: tminami@iis.u-tokyo.ac.jp

CONTENTS

1. General **S2**

2. DFT calculation **S3**

3. Cyclic voltammetry for electrochemical polymerization of NIP **S3**

4. Electrochemical quartz crystal microbalance (EQCM) **S4**

5. Differential pulse voltammetry **S5**

6. Fabrication of extended-gate type OFET **S6**

7. Selectivity study **S7**

8. Reusability study **S10**

References **S13**

1. General

Materials

3-Hydroxytyramine hydrochloride, 1,2-diaminobenzene, amino acids (L-alanine, L-(+)-arginine, L-aspartic acid, L-cysteine and L-glutamic acid), malonic acid, and taurine were purchased from Tokyo Chemical Industry Co., Ltd. Cytop (CTL809M) was supplied from Asahi Glass Co. Ltd. Polyethylene naphthalate (PEN) film, poly{2,5-bis(3-hexadecylthiophene-2-yl)thieno[3,2-*b*]}thiophene, gold, and aluminum were purchased from Teijin DuPont Films, Merck KGaA, Tanaka Kikinzoku Kogyo, Furuuchi Chemical Co., respectively. Disodium hydrogen phosphate and sodium dihydrogen phosphate were purchased from Wako Pure Chemical Industries, Ltd.

Measurements

DFT calculations were carried out in a package of Gaussian 16 REV. C. 01. Cyclic voltammetry (CV) and differential pulse voltammetry (DPV) were measured by an ALS electrochemical analyzer (600 series). Electrochemical impedance spectroscopy (EIS) was measured by an SP-300 potentiostat from Biologic. The electrical characteristics of all OFET devices were measured using a Keithley 2602B source meter. OFET devices were operated on a Manual Probe System α100 from Apollo Wave. An Au-sputtered circular 9 MHz AT-cut quartz substrates (QCM substrate, Seiko EG&G Co., Ltd., Japan) with a diameter of 5.0 mm was used to measure the resonance frequency changes of the composite electrodes with a quartz crystal microbalance (QCM). The QCM electrode was attached to a dipping-type polytetrafluoroethylene (PTFE) holder that was connected to an oscillating circuit with a

resonance frequency counter (Seiko EG&G, QCA922, Japan). Cyclic voltammetry for the QCM was performed using a potentiostat/galvanostat (Biologic SP-150Y, France).

2. DFT calculation

Table S1. The binding energy (*BE*) of the molecular complexes with different ratios calculated by M06-2X-D3(0)/ma-def2-TZVPP with PCM solvent model (water was set as a solvent).

Ratio	*BE* (raw) / kcal·mol^{-1}	*BSSE* correlation / kcal·mol^{-1}	*BE* (correlated) / kcal·mol^{-1}
1:1:1	**-15.4**	**2.5**	**-12.9**
2:1:1	**-15.1**	**3.5**	**-11.6**
3:1:1	**-53.4**	**5.3**	**-48.1**
4:1:1	**-52.2**	**6.6**	**-45.6**

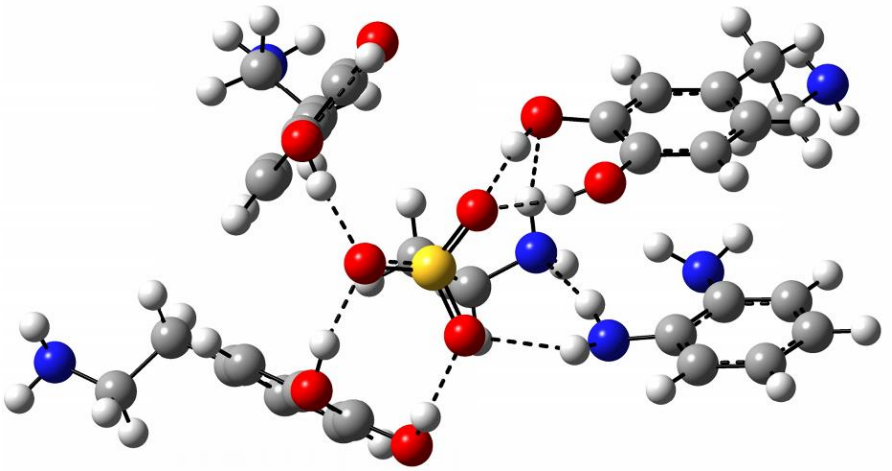

Fig. S1 The optimized structure of the molecular complex found by the M06-2X-D3(0)/ma-def2-TZVPP with the IEFPCM solvent model (solvent set as water).

3. Cyclic voltammetry for electrochemical polymerization of NIP

For electrochemical polymerization for non-imprinted polymer (NIP) by cyclic voltammetry, 3-hydroxytyramine hydrochloride (22.7 mg, 6 mM), 1,2-diaminobenzene (4.32 mg, 2 mM) were dissolved in 20 mL of PBS (20 mM) at pH 7.4. The three-electrode system (a gold film electrode as

the working electrode, an Ag/AgCl in 3 M NaCl as the reference electrode, and a Pt wire as the counter electrode) was used for the polymerization. To measure CV for the NIP, the potential range was set between −0.5 and +0.5 V (*vs.* Ag/AgCl). The scan rate was set as 0.02 V s^{-1} with the current sensitivity of 10^{-6} A. The CV measurements were repeated for 10 cycles.

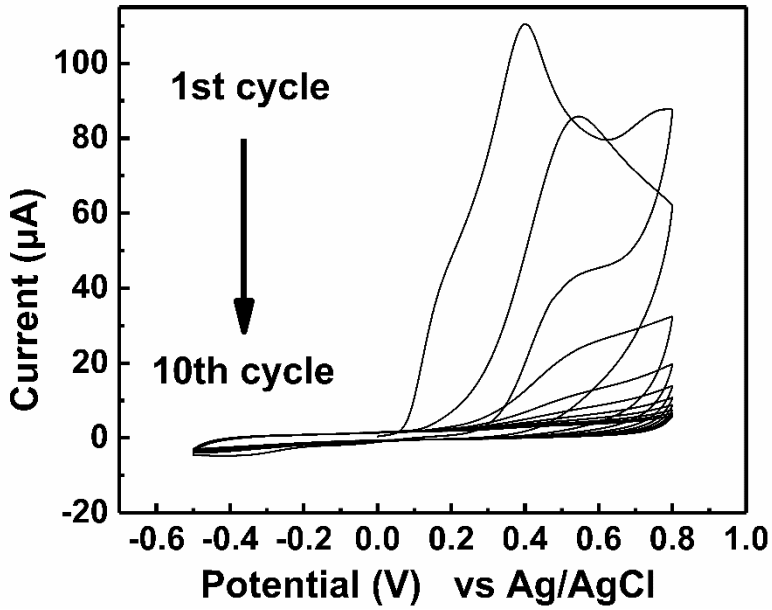

Fig. S2 Cyclic voltammograms obtained during the formation of the NIP film on the surface of Au in the PBS (20 mM) at pH 7.4 containing 6 mM dopamine and 2 mM 1,2-diaminobenzene. Scan rate: 0.02 V/s.

4. Electrochemical quartz crystal microbalance (EQCM)

Au-sputtered circular 9 MHz AT-cut quartz substrates with a diameter of 5.0 mm were used to measure the resonance frequency changes of the composite electrodes with a quartz crystal microbalance (QCM)[1]. The QCM electrode was attached to a dipping-type PTFE holder that was connected to an oscillating circuit with a resonance frequency counter. Cyclic voltammetry was performed using a potentiostat/galvanostat. The mass change (Δm) of the QCM electrode was calculated from the change in resonance frequency Δf using the Sauerbrey equation;[2]

$$\Delta m = -\Delta f\,[A(\rho_q\mu_q)^{0.5}] / (2 f_0^2)$$

where f_0 is the resonance frequency of the QCM electrode before the electrochemical tests, A is the active surface area of the QCM electrode (0.196 cm^2), ρ_q is the density of quartz (2.648 g cm^{-3}), and μ_q is the shear modulus of quartz (2.947×10^{11} g cm^{-1} s^{-2}). The mass of the electrode increased with the polymerization, and the estimated increase in the mass of MIP and NIP electrodes were estimated as 1.17 μg and 1.69 μg, respectively.

5. Differential pulse voltammetry

Differential pulse voltammetry (DPV) with a three-electrode system was applied to evaluate the response of the devices to taurine. The MIP / NIP covered gold film electrode as the working electrode, an Ag/AgCl with 3 M KCl as the reference electrode, and a Pt wire as the counter electrode were used for the measurement. The PBS solution (50 mM) with K_3FeCN_6 (50 mM) and KCl (100 mM) at pH 7.4 was used as the background solution. The potential range was set as 0.35 − 0.16 V with the scan rate of 4 mVs^{-1}. The degrees of amplitude and sensitivity were set as 50 mV and 10^{-5} A, respectively.

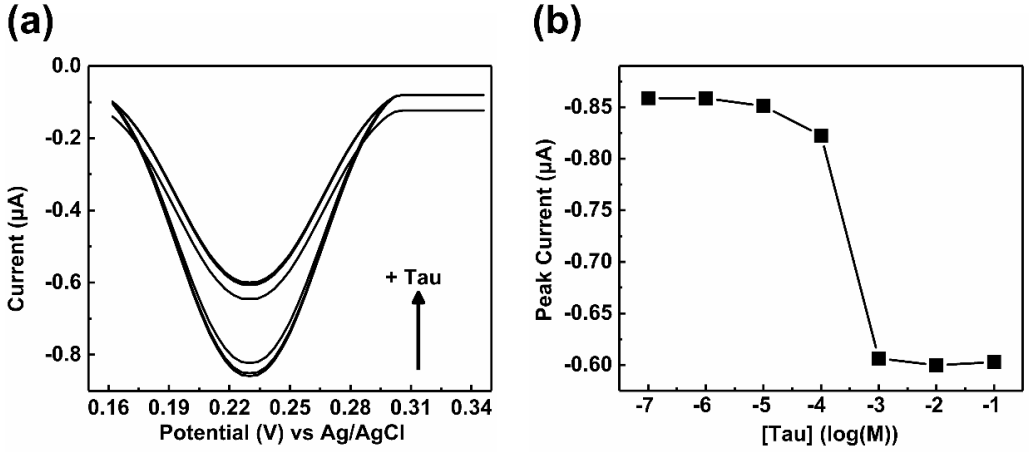

Fig. S3 (a) DPV analysis and (b) the peak current values of the MIP electrode (after extraction) toward various concentrations of taurine (10^{-7}–10^{-1} M) in the background solution.

6. Fabrication of extended-gate type OFET

The device includes two parts: the drive component (*i.e.*, OFET) and the detection component (*i. e.*, MIP extended-gate electrode) (see Fig. 1 in the manuscript). For the OFET, an Al gate electrode (30 nm in thickness) was fabricated by vacuum thermal evaporation (SVC-700TMSG/SVC-7PS80, SANYU Electron) of an Al wire and deposited on the glass substrate which was washed by a piranha solution (H_2O_2 : H_2SO_4 = 1 : 4) and Milli-Q water (18.2 Ω·cm). Reactive ion etching (RIE) (SAMCO RIE-10NR) was used for oxidizing the surface of the Al gate electrode with oxygen plasma treatment, followed by immersion of the electrode in a 2-propanol solution of tetradecylphosphonic acid (TDPA, 10 mM) for 15 h at room temperature to form an AlOx/TDPA dielectric layer (5 nm in thickness). After this period, the source and drain electrodes were deposited by vacuum thermal evaporation (30 nm in thickness) on the dielectric layer. The organic semiconductor layer (OSC) made of poly{2,5-bis(3-hexadecylthiophene-2-yl)thieno[3,2-*b*]thiophene} (PBTTT) was formed by a drop-casting method and was baked at 160 °C for 10 min. Subsequently, Cytop® (CTL-809M in CT-Solv.180, ratio 1 : 1 (v/v)) was spin-coated on the OSC layer and baked at 110 °C for 10 min to form the passivation layer. Finally, the extended gate (*i.e.*, the conductive area) (15 mm^2) was fabricated by thermal vacuum deposition of Au (100 nm in thickness).

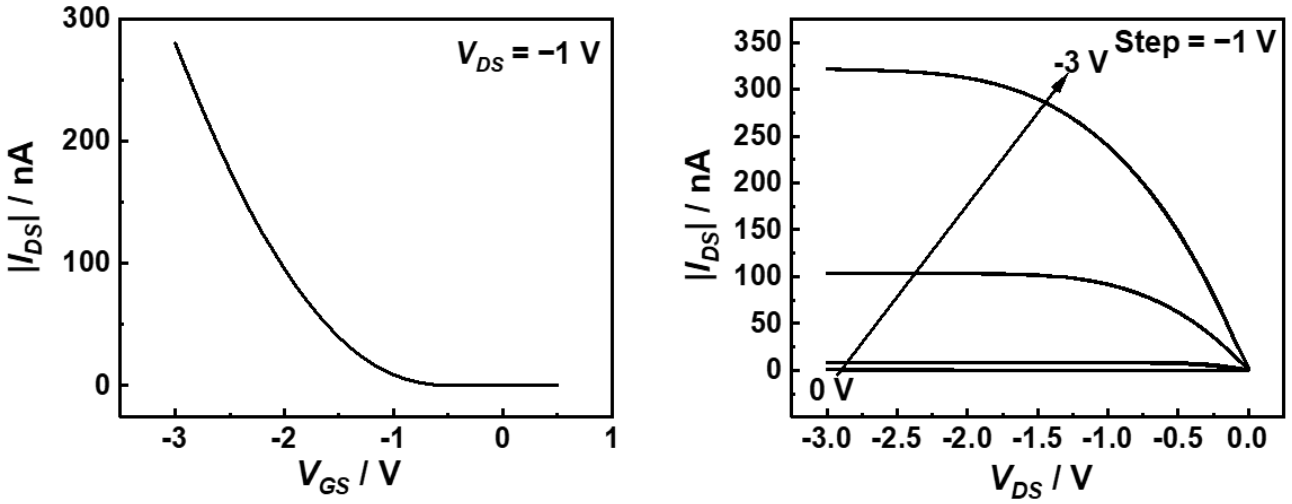

Fig. S4 Transfer (left) and output (right) characteristics of the fabricated OFET.

7. Selectivity study

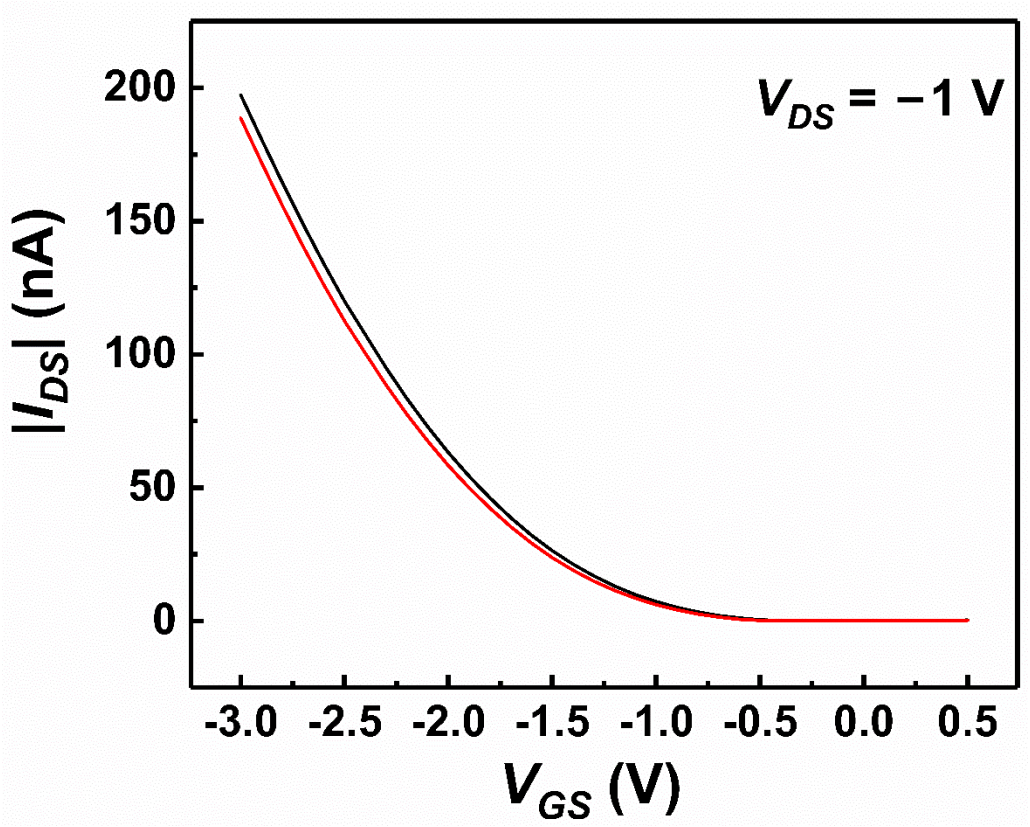

Fig. S5 Transfer characteristics of the fabricated MIP-OFET in blank solution (black line) and after adding 10 μM L-alanine (red line).

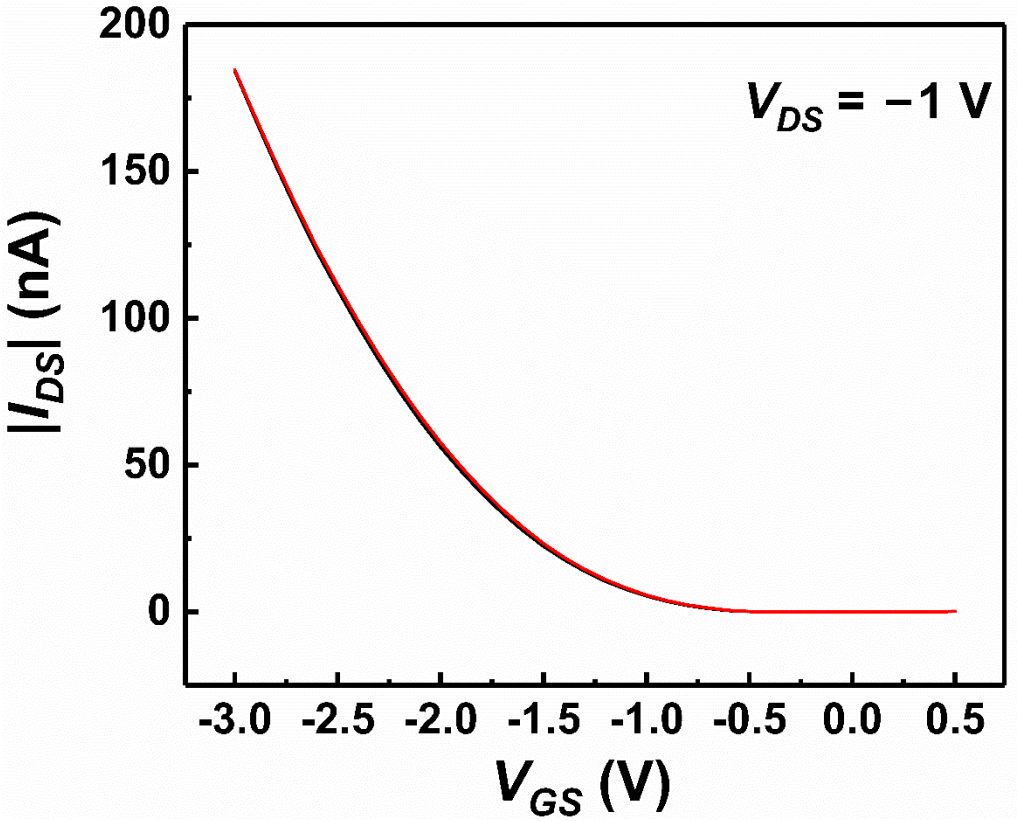

Fig. S6 Transfer characteristics of the fabricated MIP-OFET in blank solution (black line) and after adding 10 μM L-arginine (red line).

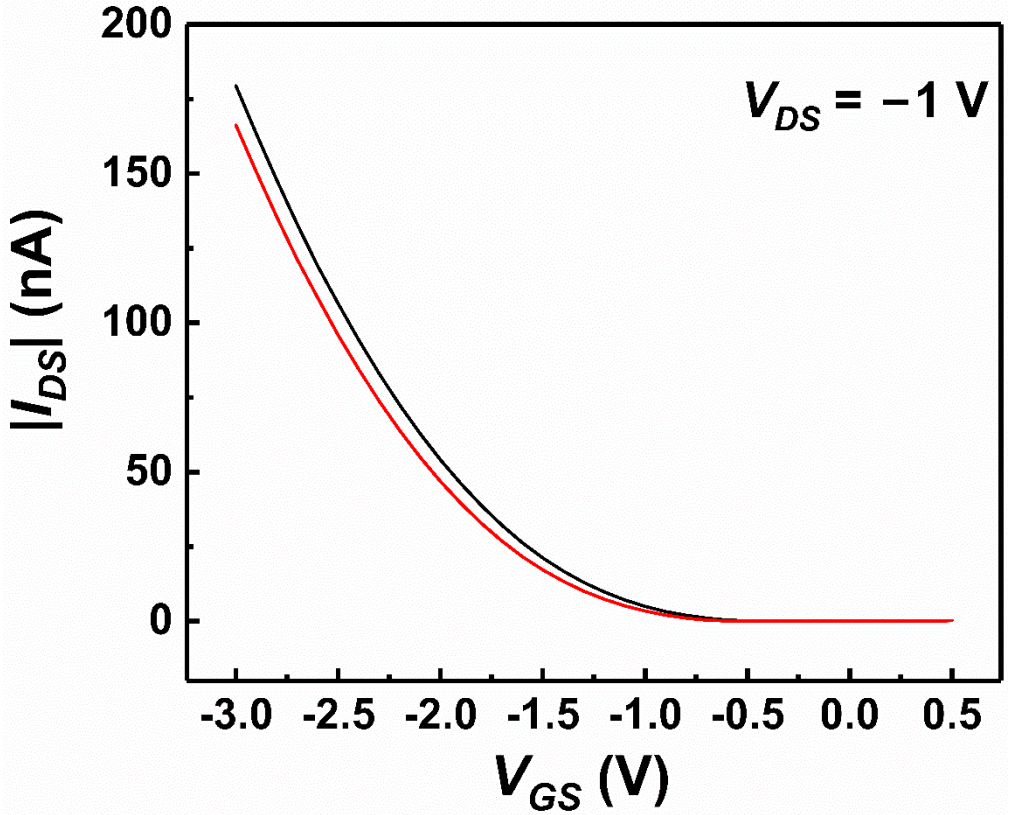

Fig. S7 Transfer characteristics of the fabricated MIP-OFET in blank solution (black line) and after adding 10 μM L-aspartic acid (red line).

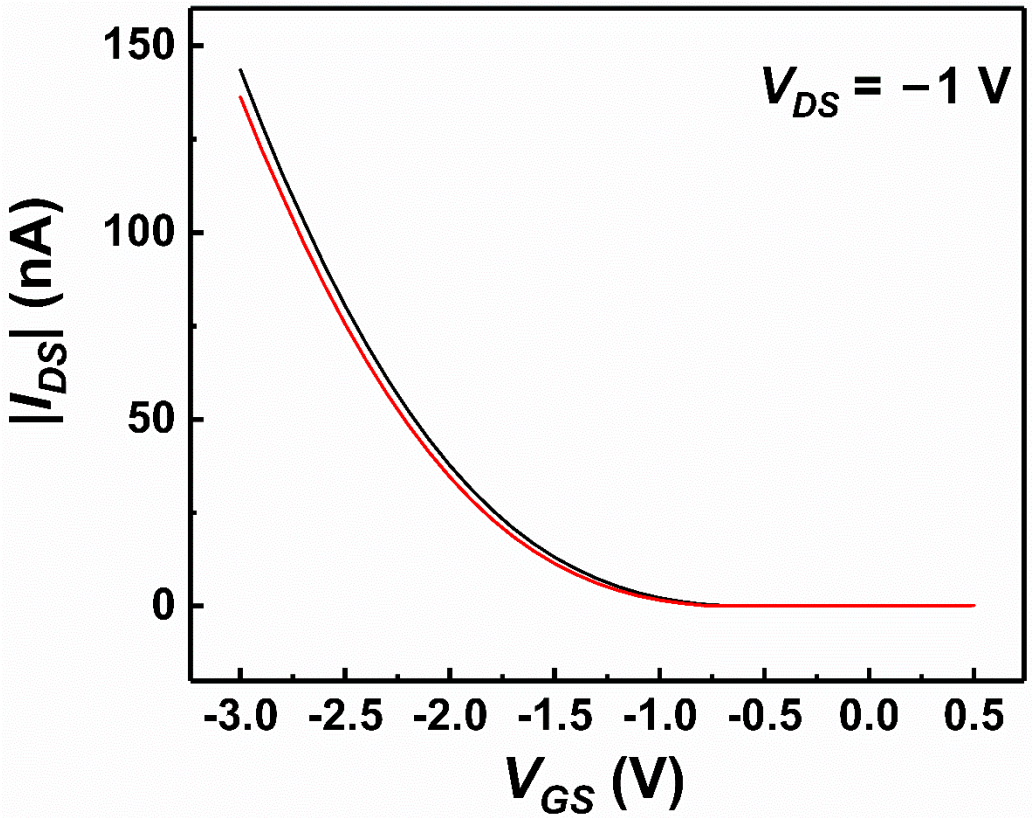

Fig. S8 Transfer characteristics of the fabricated MIP-OFET in blank solution (black line) and after adding 10 μM L-cysteine (red line).

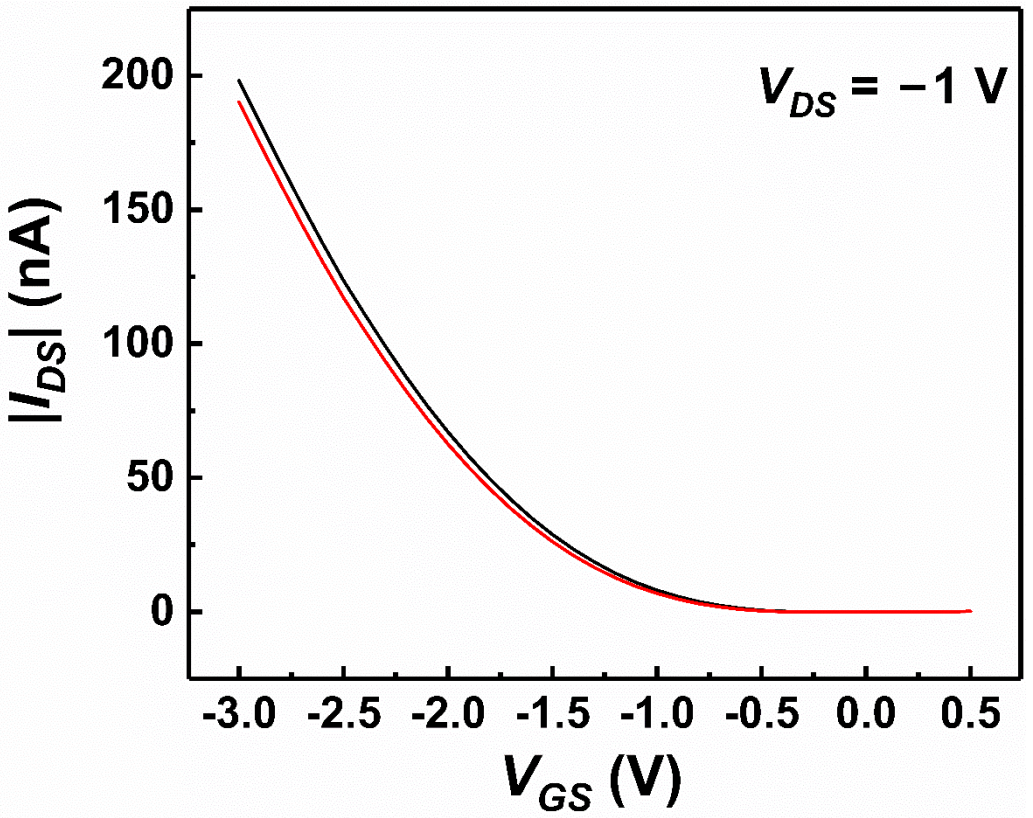

Fig. S9 Transfer characteristics of the fabricated MIP-OFET in blank solution (black line) and after adding 10 μM L-glutamic acid (red line).

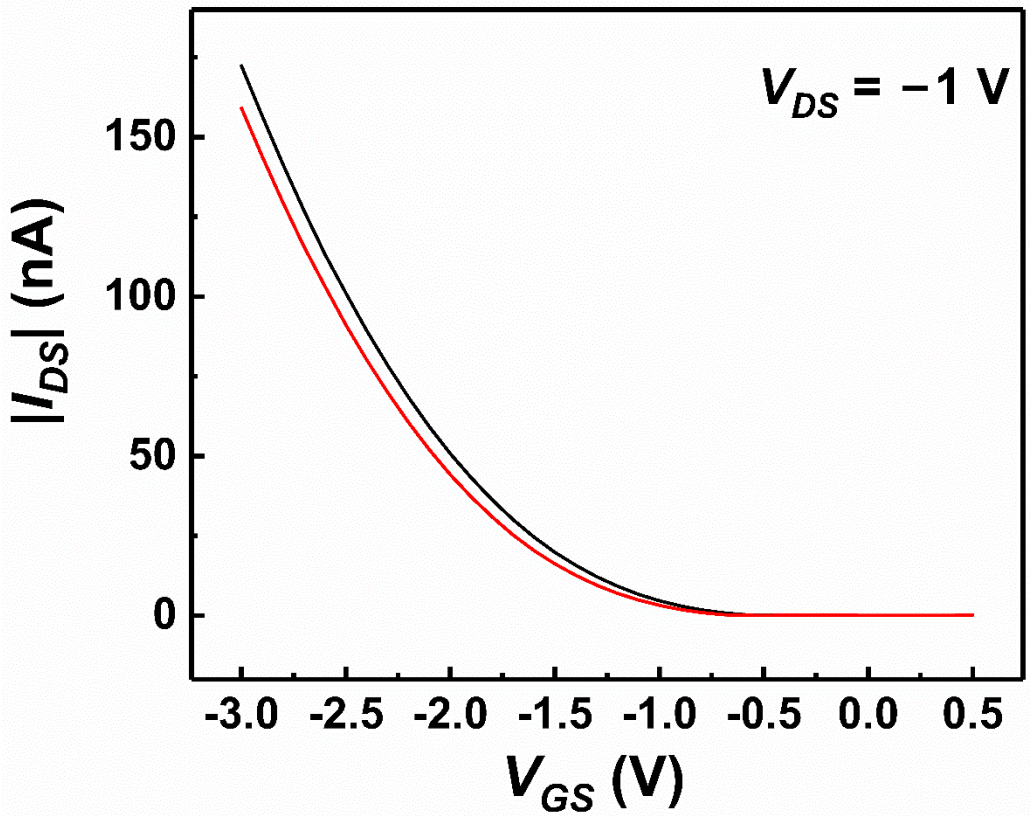

Fig. S10 Transfer characteristics of the fabricated MIP-OFET in blank solution (black line) and after adding 10 μM malonic acid (red line).

8.Reusability study

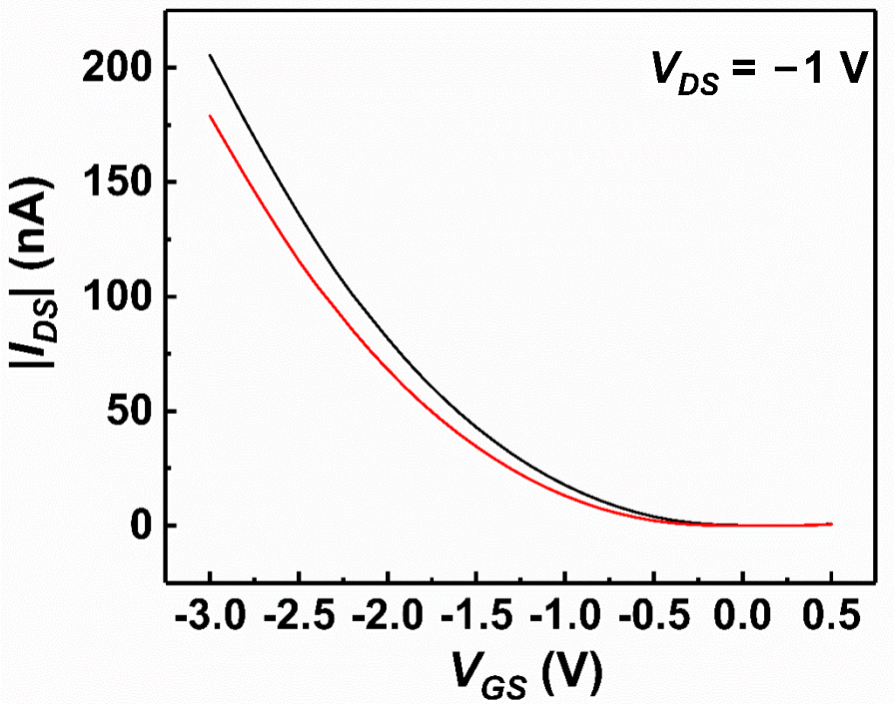

Fig. S11 Transfer characteristics of the fabricated MIP-OFET in blank solution (black line) and after adding 10 μM taurine (red line), indicating the first cycle of the reusability test.

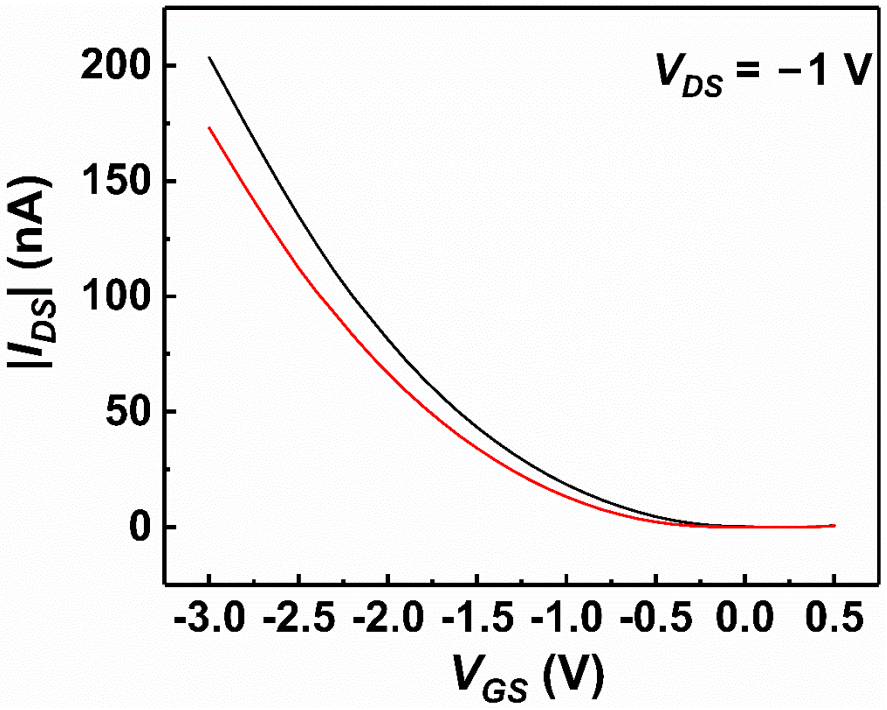

Fig. S12 Transfer characteristics of the after-washed MIP-OFET in blank solution (black line) and after adding 10 μM taurine (red line), indicating the second cycle of the reusability test.

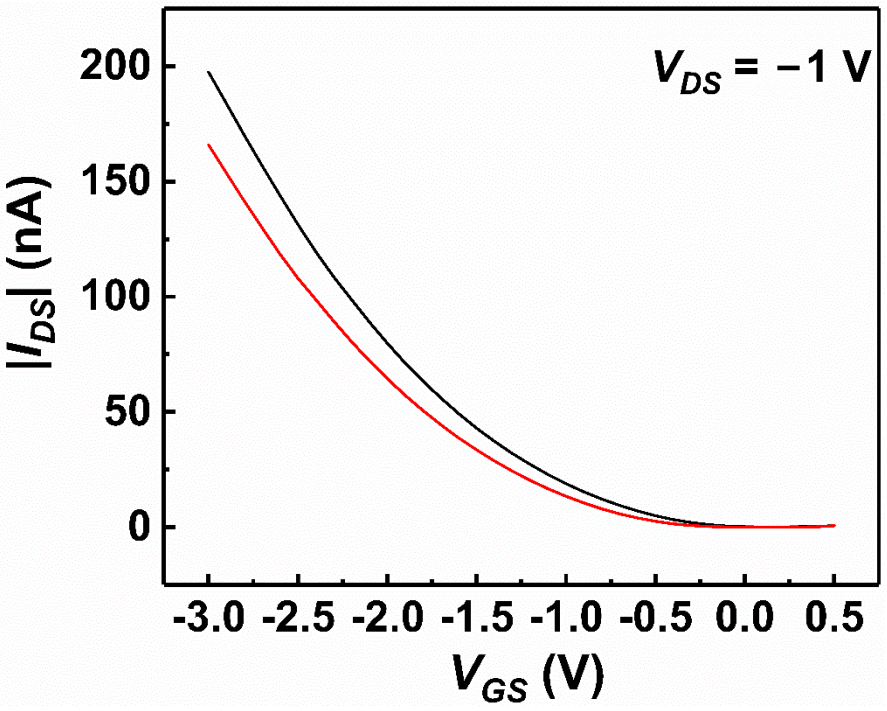

Fig. S13 Transfer characteristics of the after-washed MIP-OFET in blank solution (black line) and after adding 10 μM taurine (red line), indicating the third cycle of the reusability test.

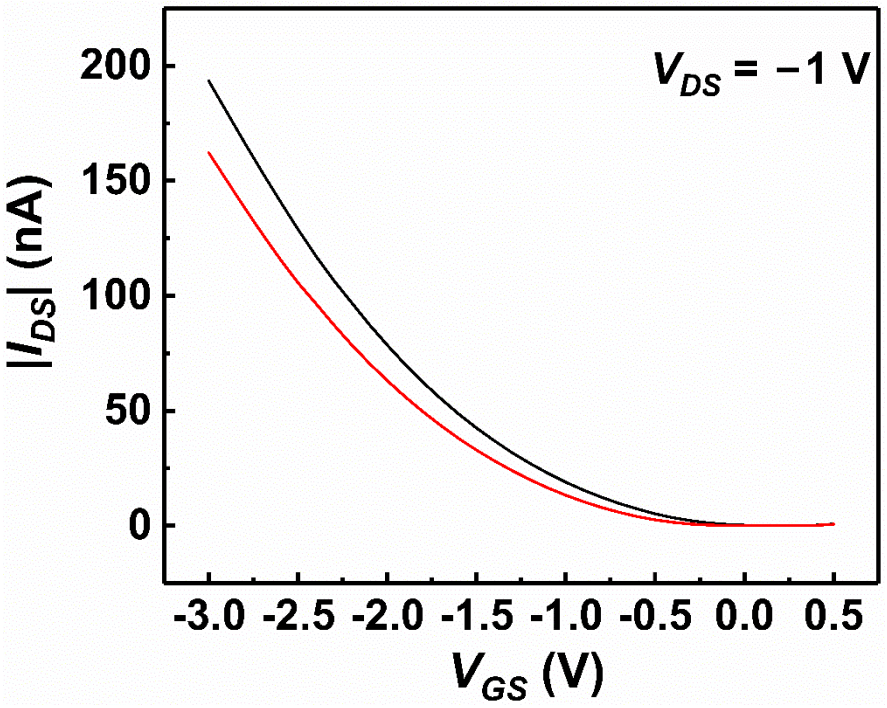

Fig. S14 Transfer characteristics of the after-washed MIP-OFET in blank solution (black line) and after adding 10 μM taurine (red line), indicating the fourth cycle of the reusability test.

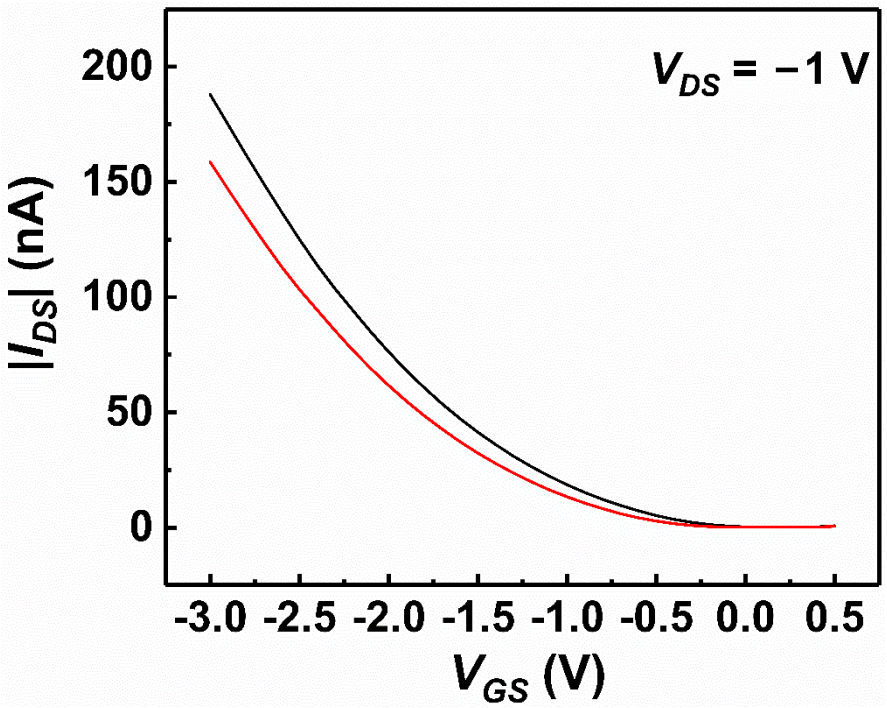

Fig. S15 Transfer characteristics of the after-washed MIP-OFET in blank solution (black line) and after adding 10 μM taurine (red line), indicating the fifth cycle of the reusability test.

References

1. S. Yagi, M. Fukuda, R. Makiura, T. Ichitsubo and E. Matsubara, *J. Mater. Chem. A*, 2014, **2**, 8041−8047.
2. G. Sauerbrey, *Z. Phys.*, 1959, **155**, 206−222.